

Glutamate-oxaloacetate transaminase activity promotes palmitate lipotoxicity in rat hepatocytes by enhancing anaplerosis and citric acid cycle flux

Robert A. Egnatchik¹, Alexandra K. Leamy^{1,‡}, Sarah A. Sacco¹, Yi Ern Cheah¹, Masakazu Shiota², Jamey D. Young^{1,2,*}

¹Chemical and Biomolecular Engineering, Vanderbilt University; Nashville, TN 37235

²Molecular Physiology and Biophysics, Vanderbilt University; Nashville, TN 37235

Running title: Role of GOT in hepatocyte lipotoxicity

[‡]Present address: University of Cincinnati College of Medicine; Cincinnati, OH 45267

*To whom correspondence should be addressed: Jamey D. Young

Phone: 615-343-4253

Fax: 615-343-7951

E-mail: j.d.young@vanderbilt.edu

Keywords: lipotoxicity, hepatocyte, anaplerosis, glutamine, fatty acid, metabolic flux analysis, tricarboxylic acid cycle (TCA cycle) (Krebs cycle), fatty liver disease

ABSTRACT

Hepatocyte lipotoxicity is characterized by aberrant mitochondrial metabolism, which predisposes cells to oxidative stress and apoptosis. Previously, we reported that translocation of calcium from the ER to mitochondria of palmitate-treated hepatocytes activated anaplerotic flux from glutamine to α -ketoglutarate (α KG), which subsequently entered the citric acid cycle (CAC) for oxidation. We hypothesized that increased glutamine anaplerosis fueled elevations in CAC flux and oxidative stress following palmitate treatment. To test this hypothesis, primary rat hepatocytes or immortalized H4IIEC3 rat hepatoma cells were treated with lipotoxic levels of palmitate while modulating anaplerotic pathways leading to α KG. We found that culture media supplemented with glutamine, glutamate, or dimethyl- α KG increased palmitate lipotoxicity compared to media that lacked these anaplerotic substrates. Knockdown of glutamate-oxaloacetate transaminase (GOT) activity significantly reduced the lipotoxic effects of palmitate, while knockdown of glutamate dehydrogenase (GluD1) had no effect on palmitate lipotoxicity. ¹³C flux analysis of H4IIEC3 cells co-treated with palmitate and the pan-transaminase inhibitor aminooxyacetic acid (AOA) confirmed that reductions in lipotoxic markers were associated with decreases in

anaplerosis, CAC flux, and oxygen consumption. Taken together, these results demonstrate that lipotoxic palmitate treatments enhance anaplerosis in cultured rat hepatocytes, causing a shift to aberrant transaminase metabolism that fuels CAC dysregulation and oxidative stress.

The liver is a central metabolic hub of the body, regulating glucose, lipid, and amino acid metabolism. As such, many hepatic pathologies are associated with altered metabolic activities. In particular, nonalcoholic fatty liver disease (NAFLD) and nonalcoholic steatohepatitis (NASH), both hepatic manifestations of the metabolic syndrome, are associated with hepatic insulin resistance and altered mitochondrial capacity including impaired fatty acid oxidation and increased anaplerosis (1-5). While plasma free fatty acid (FFA) concentrations are often elevated in these pathologies (6,7), the biochemical mediators and metabolic pathways linking elevated plasma FFAs to mitochondrial metabolic dysfunction are currently unclear. Interestingly, clinical and animal models of NASH and fatty liver have demonstrated significant alterations in plasma amino acid levels in addition to alterations of plasma FFA profiles, suggesting systemic dysregulation of amino acid metabolism (8-10).

Altered plasma glutamine and glutamate levels have previously been identified as markers in patients with metabolic syndrome and NASH (8,11). In particular, decreases in the ratio between glutamine and glutamate are associated with enhanced systemic glucose intolerance as glutamate can potentiate the formation of plasma alanine, and therefore stimulate gluconeogenesis. Additionally, abnormal glutamatyl-dipeptide synthesis has been associated with many liver diseases including NASH and hepatocellular carcinoma (12). This was attributed to inefficient synthesis of glutathione to combat oxidative stress associated with liver disease. Conversely, it has been previously hypothesized that the NAFLD biomarkers glutamate-pyruvate transaminase (GPT, or alanine aminotransferase) and glutamate-oxaloacetate transaminase (GOT, or aspartate aminotransferase) may participate in a causative mechanism of fatty liver disease progression (13).

Consistent with the hypothesis that alterations in amino acid metabolism could potentiate disease, *in vitro* models of lipotoxicity have shown that cultured hepatocytes treated with a lipotoxic load of the saturated fatty acid palmitate are characterized by altered mitochondrial metabolism involving enhanced oxidative flux and increased anaplerosis from glutamine to alpha-ketoglutarate (α KG) (14-16). Furthermore, supplementing culture media with a mixture of nonessential amino acids (NEAAs) enhanced anaplerotic flux, oxidative stress, and apoptosis markers in the presence of palmitate (14). Glutamate was identified as the single most important NEAA contributing to the observed effects (14). This finding agrees with *in vivo* studies in mice and humans which show that elevations in intrahepatic lipids are associated with increased mitochondrial anaplerosis and oxidative citric acid cycle (CAC) flux (4,5). Addition of exogenous antioxidants to cultured hepatocytes did not reverse these metabolic abnormalities, indicating that increased anaplerosis was not simply a response to oxidative stress but could play a causal role in stimulating oxidative metabolism (16). Indeed, reducing anaplerotic flux through inhibition of PEP carboxykinase (PEPCK) or treatment with metformin has been shown to prevent FFA-induced increases in oxidative stress and inflammation, both *in vitro* and *in vivo* (16,17).

We have previously demonstrated that addition of the calcium chelator BAPTA to palmitate-treated hepatic cells attenuates mitochondrial oxygen consumption, CAC anaplerosis, and oxidative stress (15). This finding suggests that alterations in intracellular calcium trafficking can predispose mitochondria to an oxidative phenotype that contributes to lipotoxicity. Calcium is a known regulator of α KG dehydrogenase (ADH) as well as the glutamate-aspartate uniporter citrin (SLC25A13), the action of which can lead to increased import and oxidation of glutamate by mitochondria. A recent study by Miller et al. (18) showed that glucagon-stimulated calcium release from the ER enhances gluconeogenesis from glutamine, which is prevented by knockdown of mitochondrial glutaminase (GLS2). Therefore, we hypothesized that glutamine anaplerosis is upregulated in response to palmitate treatment and fuels elevations in CAC flux by supplying excess α KG. As such, the deregulation of carbon entry to the CAC at the α KG node represents one potential mechanism by which calcium translocation to mitochondria can accelerate lipotoxicity.

To test the hypothesis that anaplerotic flux from glutamine to α KG modulates the severity of palmitate lipotoxicity, we altered extracellular media concentrations of glutamine, glutamate, and dimethyl- α KG to determine if the presence of these anaplerotic substrates predisposed hepatocytes to enhanced apoptosis in the presence of lipotoxic concentrations of palmitate. Additionally, we employed pharmacologic inhibition and siRNA-mediated knockdown of the GOT and glutamate dehydrogenase (GluD1) pathways of α KG anaplerosis (Figure 1). We found that knockdown of GOT activity, but not GluD1, significantly decreased hepatic lipoapoptosis in primary rat hepatocytes and immortalized H4IIEC3 rat hepatoma cells. Pharmacologic inhibition of transaminase metabolism using the pan-transaminase inhibitor aminooxyacetic acid (AOA) attenuated the enhancement of oxygen uptake we have previously reported as a characteristic of palmitate lipotoxicity in hepatocyte cultures (15,16). Similarly, ^{13}C flux analysis revealed that AOA reduced absolute rates of glutamine anaplerosis and CAC flux compared to cells treated with palmitate alone. Taken together, these results indicate that palmitate treatment stimulates GOT-

dependent anaplerosis to supply α KG and downstream CAC intermediates. When uninhibited, this mechanism leads to metabolic dysfunction and oxidative stress associated with hepatocyte lipotoxicity (15,16).

RESULTS

Extracellular glutamine enhances palmitate lipotoxicity of rat hepatocytes—We have previously shown that glutamine anaplerosis is increased independently of caspase 3/7 activity in palmitate-treated H4IIEC3 cells (19). However, the effects of glutamine removal or replacement on palmitate-induced lipotoxicity have not been systematically assessed. To test that exogenous glutamine enhances apoptosis, primary rat hepatocytes or H4IIEC3 rat hepatoma cells were treated with 400 μ M palmitate in the presence or absence of 2 mM glutamine. Removal of extracellular glutamine attenuated cell death associated with palmitate treatment (Figure 2A). Additionally, the reduction in palmitate-induced lipotoxicity of H4IIEC3 cells was associated with a reduction in markers of apoptosis (Figure 2B).

The metabolic products of glutamine anaplerosis promote lipotoxic cell death of rat hepatocytes—Glutamine can be metabolized via conversion to glutamate and then to the CAC intermediate α KG (Figure 1). If glutamine fuels lipotoxicity by providing substrates for mitochondrial anaplerosis, its direct downstream metabolites should also stimulate hepatocyte cell death in response to elevated doses of palmitate. To test this hypothesis, primary rat hepatocytes or H4IIEC3 cells were treated with 400 μ M palmitate and incubated with 2 mM glutamine, 2 mM glutamate, or 2 mM α -ketoglutarate (using the cell-permeable analog dimethyl- α KG) for 24 hours. H4IIEC3 cells exhibited identical toxicity responses to palmitate under all media conditions, indicating that these metabolites act as interchangeable substrates for promoting mitochondrial phenotypes associated with lipotoxicity (Figure 3A). Interestingly, primary hepatocytes exhibited increased lipotoxic cell death when extracellular glutamine was replaced with glutamate or α -ketoglutarate. This trend suggests that primary hepatocytes have enhanced sensitivity to downstream glutamine-derived anaplerotic substrates than to glutamine itself. This could be

due to reduced glutaminase activity in primary hepatocytes, which is needed to convert glutamine to glutamate. Our primary hepatocyte isolation homogenizes the entire liver, producing a mixed population of hepatocytes. However, glutaminase is only expressed in a narrow layer of hepatocytes surrounding the periportal vein (20). This could explain why glutamate and α KG are more synergistic than glutamine in primary hepatocytes (21,22).

Glutamate can produce α KG through direct deamination by glutamate dehydrogenase (GluD1) or through transamination to produce NEAAs such as alanine or aspartate. Of particular interest is the glutamate-oxaloacetate transaminase (GOT) family of enzymes, since they play a key role in the malate/aspartate shuttle, a critical redox shuttle whose activity can be influenced by alterations in intracellular calcium (23,24). GOT catalyzes the conversion of glutamate to α KG via the transamination of oxaloacetate to aspartate. Since we have previously observed calcium-dependent anaplerosis in palmitate-treated hepatic cells (15), we hypothesized that GOT metabolism could be the primary route of anaplerosis that is upregulated in response to palmitate treatment. To test this hypothesis, hepatocytes were treated with 400 μ M palmitate and provided either extracellular glutamine or a combination of α KG and aspartate. Both primary hepatocytes and H4IIEC3 cells exhibited enhanced lipotoxic cell death when given the mixture of GOT products rather than glutamine alone (Figure 3B). These results are in agreement with a previous finding that supplementation of exogenous glutamate, or mixtures of NEAAs, accelerated lipotoxic ROS generation and apoptosis of palmitate-treated H4IIEC3 cells (14).

The GOT family of enzymes promotes lipotoxicity in rat hepatocytes—The observation that products of GOT metabolism enhanced lipotoxicity in both H4IIEC3 cells and primary rat hepatocytes suggests that GOT enzymes play an important role in providing anaplerotic substrates to fuel CAC activation in response to palmitate treatments. Thus, we utilized siRNA to selectively modulate glutamate dehydrogenase or GOT metabolic activities in order to assess these alternative pathways of glutamate anaplerosis. First, we knocked down mRNA expression of glutamate dehydrogenase using siRNA specific for

Glud1 in H4IIEC3 cells. Knockdown of Glud1 had no effect on palmitate-induced apoptosis, indicating that Glud1 is not a primary metabolic pathway that potentiates lipotoxicity in H4IIEC3 cells (Figure 4A). Next, we used siRNA for both the cytosolic and mitochondrial isoforms of GOT, GOT1 and GOT2, respectively. Compared to H4IIEC3 cells treated with a control siRNA (NC1), GOT1 siRNA significantly attenuated caspase activity by approximately 25% after 12 hours of palmitate treatment (Figure 4B). Interestingly, GOT2 knockdown attenuated palmitate-induced apoptosis even more effectively than GOT1 knockdown (Figure 4C). When we repeated these experiments using primary rat hepatocytes, we found that Glud1 and GOT1 knockdown produced no significant improvements in lipotoxicity markers (not shown), but GOT2 knockdown produced a reduction in palmitate-induced apoptosis that was similar to that observed in H4IIEC3 cells (Figure 4D).

AOA co-treatment attenuates palmitate-induced cell death and oxygen consumption in H4IIEC3 cells—We have previously shown that lipotoxic concentrations of palmitate induce metabolic dysfunction characterized by elevated anaplerosis and oxygen consumption flux in H4IIEC3 cells (19). To further explore the metabolic impacts of GOT inhibition, we used the pan-transaminase inhibitor aminooxyacetic acid (AOA) to suppress glutamate-dependent anaplerosis. Co-treatment of H4IIEC3 cells with 400 μ M palmitate and 500 μ M AOA resulted in a 50% reduction in palmitate-induced cell death (Figure 5A), which was associated with a proportional reduction in palmitate-induced oxygen consumption (Figure 5B). These results indicate that the mechanism of AOA-mediated suppression of lipotoxicity may be linked to the ability of AOA to partially reverse mitochondrial metabolic alterations associated with palmitate treatment.

Transaminase inhibition by AOA reverses palmitate-induced alterations in CAC-associated metabolic fluxes—To examine how AOA confers resistance to palmitate treatments in H4IIEC3 cells, we performed ^{13}C metabolic flux analysis (MFA) by complete replacement of medium glutamine with the stable isotope tracer $[\text{U}-^{13}\text{C}_5]\text{glutamine}$. Labeled intracellular metabolites were extracted and analyzed for isotopic enrichment using GC-

MS. Previously, we observed that palmitate-treated cells incorporated more $[\text{U}-^{13}\text{C}_5]\text{glutamine}$ -derived carbon into CAC intermediates (e.g., malate) relative to vehicle-treated cells, as quantified by their atom percent enrichment (APE) (16). AOA co-treated cells exhibited less ^{13}C enrichment in the aspartate pool, indicating that transaminase activity was effectively inhibited (Figure 6A). Additionally, compared to palmitate-treated cells, the malate enrichment was significantly lower in cells co-treated with AOA. Despite these differences, the isotopic enrichment of the glutamate pool was only modestly decreased, suggesting that glutamate synthesis from extracellular glutamine was largely unaffected by AOA co-treatment. Interestingly, co-treating cells with AOA and palmitate increased the APE of both lactate and phosphoenolpyruvate (PEP) compared to cells treated with palmitate alone (Figure 6B). This indicates a re-routing of cataplerotic flux leaving the CAC via PEPCK.

Next, we performed ^{13}C MFA by applying a metabolic model consisting of key glycolytic and CAC reactions (Figure 7A, SI Table S1) to regress fluxes from measured isotope labeling patterns of several GC-MS fragment ions (SI Table S2). The model was constrained by mass balances on all network metabolites, isotopomer balances on all relevant elementary metabolite units, and redox balances on NADH and FADH₂. Fluxes were estimated by least-squares regression of nine measured mass isotopomer distributions (MIDs) (SI Figures S1–S3) in combination with the measured oxygen uptake rates shown in Figure 5B. We calculated 14 net fluxes for H4IIEC3 cells treated with vehicle, palmitate (PA), or a combination of palmitate and AOA (SI Tables S3–S5). Consistent with our prior studies (14–16), we observed significant elevations in glutaminase (GLS), citrate synthase (CS), α -ketoglutarate dehydrogenase (ADH), and malic enzyme (ME) fluxes in response to palmitate treatment (Figure 7B). AOA co-treatment led to significant reductions in GLS, ADH, and ME fluxes compared to cells treated with palmitate alone, although GLS and ADH fluxes remained elevated in comparison to vehicle-treated cells. However, no significant difference was observed in the CS flux of cells treated with PA versus PA+AOA, indicating that

AOA was not able to reverse all aspects of palmitate-induced CAC dysregulation.

In addition to increasing the utilization of glutamine-derived carbon by enhancing GLS flux, palmitate treatment also increased utilization of glucose-derived carbon as indicated by elevations in pyruvate kinase (PK) flux (Figure 7C). Unlike GLS flux, however, PK flux was completely restored to basal levels by AOA co-treatment. Normalizing the intracellular fluxes to PK demonstrates that the palmitate-induced mitochondrial alterations were associated with enhanced glutamine anaplerosis and a decrease in pyruvate carboxylase (PC)-dependent CAC anaplerosis (Figure 7D). Interestingly, although AOA co-treatment reduced absolute CAC fluxes, the relative ratios of GLS/PK, CS/PK, and ADH/PK fluxes were elevated compared to vehicle-treated cells. This observation suggests that the use of glutamine as a carbon source for the CAC remains elevated compared to glucose, despite inhibition of transaminase activity by AOA.

Net anaplerotic flux into the CAC must balance net cataplerotic flux leaving the cycle during metabolic steady state (21). In our previous studies (14-16), glutamine carbon entering the CAC as α -ketoglutarate was postulated to leave through either malic enzyme or CO_2 production. Here, our updated model includes the PEPCK reaction, which exhibited low flux in both vehicle-treated and palmitate-treated cells, indicating that PEPCK was not the preferred route of cataplerosis in H4IIEC3 cells cultured with abundant glucose and no added hormones (Figure 7B). Instead, flux through malic enzyme was the main mode of cataplerosis. On the other hand, AOA co-treatment was marked by a significant increase in PEPCK flux compared to cells treated with palmitate alone (Figure 7B and 7D). This partial shift from ME- to PEPCK-dependent cataplerosis could indicate intracellular accumulation of oxaloacetate due to disruption of transaminase metabolism (Figure 8).

DISCUSSION

Hepatic lipotoxicity in H4IIEC3 cells is characterized by enhanced CAC anaplerosis, which can be derived from extracellular glutamine that is abundant in cell culture media and blood plasma (typically higher than any other amino acid) (14,19). However, it is unclear whether this

anaplerotic flux is mediated solely by glutamate dehydrogenase or glutamate transaminase enzymes, and whether inhibition of these glutamate-dependent anaplerotic pathways would fully suppress metabolic phenotypes associated with FFA lipotoxicity. In the current study, we altered media glutamine concentrations to define a mechanism by which extracellular glutamine controls the rate of palmitate-induced apoptosis in H4IIEC3 rat hepatoma cells and primary rat hepatocytes. Replacing extracellular glutamine with its downstream metabolic products (e.g., glutamate, α -ketoglutarate, etc.) revealed that glutamine exerts its pro-apoptotic effects by enhancing mitochondrial anaplerosis and not simply through the accumulation of other metabolic byproducts. A similar effect has also been observed in activated macrophages: glutamine deficiency partially rescued cells from palmitate lipotoxicity, while the addition of α -ketoglutarate to the culture medium restored the lipotoxic effects of palmitate (25). While a glutamine concentration (2 mM) higher than physiological plasma levels (0.4–0.7 mM) was used in the current study, this concentration is consistent with previous lipotoxicity studies of cultured hepatocytes and other cell types (26-28). Additionally, similar results were obtained in a prior study that used physiological concentrations of glutamine (14). A superphysiological glutamine concentration was chosen to avoid glutamine depletion during the course of our experiments, which has been shown to cause a switch in metabolism from glutamine consumption to glutamine secretion at concentrations below 0.4 mM (29).

In our current study, inhibition of glutamate conversion to α -ketoglutarate using siRNA specific for Glud1, GOT1, or GOT2 indicated that glutamine enhances palmitate lipotoxicity through GOT activity, primarily through GOT2. Pharmacological transaminase inhibition with AOA confirmed these results and enabled the intracellular fate of glutamine carbon to be traced using $[\text{U-}^{13}\text{C}_5]\text{glutamine}$ labeling. Commensurate with a partial rescue in lipotoxic cell death, AOA co-treatment attenuated the metabolic dysregulation caused by palmitate treatment but did not fully restore CAC-associated fluxes to basal levels. Overall, these results demonstrate a novel role for GOT enzymes in promoting palmitate

lipotoxicity, which depends on their ability to provide substrates for CAC anaplerosis. Our study also confirms and extends the previous work of Noguchi et al. (14), which found that NEAA supplementation exacerbated the effects of PA treatment to inhibit glycolytic flux, increase CAC flux, and stimulate ROS accumulation in H4IIEC3 cells. In particular, glutamate addition induced ROS generation and apoptosis more effectively than any other single amino acid, suggesting that the stimulatory effects of NEAA supplementation could be due to enhanced glutamate anaplerosis. Our current study offers further evidence supporting that hypothesis, and provides a mechanistic description of the enzymes and pathways involved.

Alterations in amino acid metabolism have been linked to obesity, NAFLD, and NASH (8,10). In particular, elevated plasma glutamate/glutamine levels have been reported as a potential risk factor for NAFLD. Additionally, in the methionine-choline deficient (MCD) diet-induced murine NASH model, increases in plasma glutamate and glutamine were paralleled by increases in liver concentrations of these amino acids (8). The authors attributed these elevations to inhibition of liver gluconeogenesis and CAC metabolism in MCD-fed mice. In contrast, a different study demonstrated that mice fed a high-fat diet developed fatty liver and insulin resistance that is associated with increases in CAC and gluconeogenic fluxes (4). Our models of lipotoxicity in isolated rat hepatocytes and the H4IIEC3 cell line exhibit similarities with these two *in vivo* studies. First, palmitate overload induces mitochondrial dysfunction characterized by elevated CAC flux. Second, the presence of elevated glutamine or downstream glutamine-derived metabolites (e.g., glutamate or α -ketoglutarate) synergizes with palmitate to enhance lipotoxicity.

Anaplerosis of α -ketoglutarate into the CAC can occur through Glud1, cytosolic GOT1, and mitochondrial GOT2. To further examine the differences between Glud1 and GOT isoforms, hepatic cells were treated with a combination of α -ketoglutarate and aspartate (metabolic products of the GOT enzymatic reaction). The combined dose of extracellular α -ketoglutarate and aspartate supplied to palmitate-treated cells was more toxic

than glutamine alone. We then applied siRNA for Glud1, GOT1, or GOT2 to specifically inhibit these enzymes. Knockdown of GOT1 or GOT2 attenuated palmitate-dependent apoptosis in H4IIEC3 cells, while only GOT2 knockdown partially rescued apoptosis in primary rat hepatocytes. The inability of Glud1 to reduce the toxic effects of palmitate indicates that glutamate dehydrogenase likely does not play an important role in glutamate anaplerosis under these conditions. Interestingly, Glud1 activation has been shown to improve hepatic steatosis in mice fed a high-fat, high-fructose diet. It was proposed that this effect is due to reductive amination, which shunts intermediates away from the CAC and into amino acid synthesis. This opposing role of Glud1 is further evidence that decreased CAC anaplerosis can decrease the effects of lipotoxicity (30).

Both cytosolic GOT1 and mitochondrial GOT2 are reversible reactions that convert an amino acid (glutamate or aspartate) to an α -ketoacid (α -ketoglutarate or oxaloacetate). Additionally both are involved in the malate-aspartate shuttle, which functions to transport cytosolic reducing equivalents (NADH) to the mitochondria to be used for oxidative phosphorylation (Figure 8). In principle, upregulated GOT activity can therefore account for the increased oxygen consumption exhibited by palmitate-treated hepatic cells by providing more α -ketoglutarate for CAC oxidative metabolism or by shuttling more reducing equivalents into the mitochondria via the malate-aspartate shuttle. However, the latter mechanism implies a synergy between both GOT1 and GOT2 that we do not observe in our experiments. While knockdown of either GOT1 or GOT2 attenuated lipotoxicity, GOT1 knockdown had a smaller effect on H4IIEC3 cells and no significant effect in primary rat hepatocytes. This suggests that disruption of GOT2 metabolism during palmitate overload leads to increased net anaplerosis rather than simply an acceleration of substrate cycling between GOT1 and GOT2.

In addition to siRNA-mediated knockdowns, we co-treated hepatic cells with the transaminase inhibitor AOA in the presence of a lipotoxic palmitate load. AOA co-treatment attenuated lipotoxicity to a similar extent as GOT2 knockdown in H4IIEC3 cells. It is important to note that AOA inhibits multiple transaminases, so its impact is not

limited to GOT. ^{13}C MFA studies demonstrated that AOA significantly decreased glutamine anaplerosis, oxygen consumption, and ADH flux, all of which are characteristic of palmitate overload in hepatic cells. However, cells co-treated with AOA and palmitate still exhibited elevated mitochondrial fluxes in comparison to vehicle-treated cells. This failure to completely normalize mitochondrial fluxes with AOA suggests an upstream mechanism that predisposes hepatic cells to a glutamine/glutamate avid state in response to palmitate treatment.

Previously, we demonstrated a novel role for intracellular calcium to promote lipotoxicity by inducing metabolic dysfunction and oxidative stress (15). In that study, co-treating hepatic cells with palmitate and the intracellular calcium chelator BAPTA decreased mitochondrial metabolism as indicated by reduced oxygen consumption flux and decreased glutamine uptake compared to cells treated with palmitate alone. Additionally, BAPTA co-treated cells had reduced equilibration of isotope labeling in the malate and aspartate pools. These results pointed to a novel, putative role for the glutamate-aspartate antiporter citrin to enhance lipotoxicity. The activity of this antiporter is enhanced by elevations in cytosolic calcium, which may increase glutamate entry into the mitochondria in exchange for aspartate (24). Hypothetically, the net result of citrin activation in the context of palmitate lipotoxicity could be an enhancement in oxygen consumption and glutamate anaplerosis as a result of increased substrate supply to GOT2 (Figure 8). Combined with the observation that the pan-transaminase inhibitor AOA reduced oxygen consumption, aspartate labeling, and overall CAC flux in palmitate-treated cells, we hypothesize that palmitate overload exerts its lipotoxic effects through calcium-dependent activation of mitochondrial glutamate transport and GOT2-dependent anaplerosis that together fuel elevated CAC metabolism.

One potential limitation of this study is the use of ethanol in the preparation of palmitate-BSA stock solutions. In order to achieve consistent palmitate concentrations, we found that preparation with ethanol was the best method to ensure complete dissolution of palmitate and avoid its spontaneous precipitation. While the final ethanol

concentration of the palmitate incubations was less than 0.2% by volume, ethanol was still present at a level that could induce metabolic perturbations in hepatocytes due to alcohol dehydrogenase activity (e.g., accumulation of acetate in the culture medium and hyper-reduction of the NADH/NAD⁺ redox ratio). Despite this potential limitation, our findings are consistent with prior studies that did not use ethanol in their fatty acid solutions (14,26). In particular, the prior study by Noguchi et al. (14) performed ^{13}C -glutamine labeling studies in H4IIEC3 cells and also observed elevated CAC flux and increased glutaminolysis in response to palmitate treatments. Furthermore, our vehicle control (BSA) treatments contained the same amount of ethanol as the palmitate treatments. Finally, an experiment to measure the consumption of ethanol by H4IIEC3 cells showed no differences in ethanol time courses between cell-free versus cell-containing incubations and no differences in ethanol or acetate concentrations between cell cultures incubated with vehicle versus palmitate (Fig. S5). These data indicate that the rate of ethanol conversion by H4IIEC3 cells was negligible compared to cell-free controls and that changes in medium acetate concentration cannot explain the metabolic or isotopic alterations observed in response to palmitate treatment. Therefore, we have no evidence that ethanol in our fatty acid stocks was an important determinant of lipotoxicity in our studies. In addition, the use of ethanol to prepare fatty acid solutions is common throughout the lipotoxicity literature (27,28,31-34).

The results of our study suggest potential therapeutic strategies to combat the progression of NASH through inhibition of mitochondrial transaminase or glutaminase activities, or blocking transport of glutamate and glutamine into liver mitochondria. Interestingly, Miller et al. (18) have recently proposed that inhibition of mitochondrial glutaminase (GLS2) in the liver could provide a new therapeutic avenue to treat hyperglycemia in type 2 diabetes through reduction of calcium-dependent glutamine anaplerosis. Another recent study found that including plasma glutamate concentrations in a non-invasive diagnostic assay of NASH provided a more accurate diagnosis than clinical biomarkers alone (35). Therefore, improved understanding of how glutamine anaplerosis promotes hepatic lipotoxicity and

metabolic dysfunction in the context of obesity could lead to novel therapeutic or diagnostic strategies to treat NAFLD and NASH in the clinic, as well as possible dietary interventions to prevent NASH progression.

EXPERIMENTAL PROCEDURES

Reagents and chemicals—Dulbecco's modified Eagle's medium (DMEM), aminooxyacetic acid (AOA), dimethyl- α KG, aspartic acid, glutamic acid, bovine serum albumin (BSA), and palmitate were purchased from Sigma (St. Louis, MO, USA). Propidium iodide was obtained from Invitrogen (Carlsbad, CA, USA). Primary hepatocytes were cultured on plates coated with Collagen I (Rat Tail) from BD Biosciences (San Jose, CA).

Primary rat hepatocyte isolation—Primary hepatocytes were isolated from male Sprague-Dawley rats as described previously (36). The portal vein and inferior vena cava of anesthetized animals were cannulated and perfused with 37°C oxygenated perfusion medium, pH 7.4, containing 118 mM NaCl, 5.9 mM KCl, 1.2 mM MgSO₄, 1.2 mM NaH₂PO₄, 25 mM NaHCO₃, 0.2 mM EGTA and 5 mM glucose. After 15 minutes, the liver was excised from the animal and perfused with liver digest medium (Invitrogen, Grand Island NY). Then the cells were dispersed, washed four times, and suspended in attachment medium, which consisted of high-glucose DMEM supplemented with 30 mg/L proline, 100 mg/L ornithine, 0.544 mg/L ZnCl₂, 0.75 mg/L ZnSO₄ 7H₂O, 0.2 mg/L CuSO₄ 5H₂O, 0.25 mg/L MnSO₄, 2 g/L BSA, 5 nM insulin, 100 nM dexamethasone, 100,000 U penicillin, 100,000 U streptomycin, and 2 mM glutamine. After four hours of incubation in the attachment medium, hepatocytes were switched to a maintenance medium identical to the attachment medium except it had a concentration of 1 nM (instead of 5 nM) insulin.

H4IIEC3 cell culture—The H4IIEC3 rat hepatoma cell line was purchased from ATCC (American Type Culture Collection, Manassas, VA, USA). Cells were cultured in low-glucose (1 g/L) DMEM with 10% FBS, 1% penicillin/streptomycin antibiotic solution, and a basal glutamine concentration of 2 mM. For measurements of toxicity and apoptosis, cells were plated at a density of 2×10^4 cells per well in a 96-well plate and allowed to grow for two days (until

confluent) prior to the experiment. Twelve hours prior to other measurements, cells were switched to FBS-free, low-glucose DMEM supplemented with Serum Replacement 3 (Sigma).

Preparation of palmitate solutions—Stock solutions were prepared by complexing palmitate to fatty acid free BSA ($\geq 96\%$ pure). Six grams of BSA were allowed to dissolve in 1X PBS and were adjusted to a final volume of 30 mL. This 20% BSA solution was dialyzed using a 3.5 K MWCO Slide-A-Lyzer G2 Dialysis cassette (Thermo Scientific, Waltham, MA) in a 1X PBS solution. The 1X PBS solution was changed 3 times a day for 3 days. At the end of the dialysis, BSA concentration was measured and the solution was adjusted to a final concentration of 10% BSA, sterile filtered, and aliquoted.

Palmitate was dissolved in pure ethanol at a concentration of 195 mM. This solution was then added to a prewarmed 10% w/w BSA solution (37°C) to achieve a final palmitate concentration of 3 mM, and this solution was allowed to incubate in a water bath for an additional 10 minutes. The final ratio of palmitate to BSA was 2:1. All vehicle treatments were prepared using stocks of 10% w/w BSA with an equivalent volume of ethanol added to match the concentration in palmitate stocks. The final concentration of ethanol in all experimental treatments was less than 0.2% by volume. Palmitate concentrations used to induce lipotoxicity were consistent with previous studies (26,31-33,37,38).

Toxicity assays—Losses in cell viability in response to palmitate treatments were assessed using the dead-cell stain propidium iodide (PI). The intercalating dye becomes highly fluorescent when bound to exposed double-stranded DNA of dead cells. Fluorescence was assessed using excitation wavelength of 530 nm and emission wavelength of 645 nm with a BioTek Cytation 3 plate reader.

Caspase activity—Caspase activity was measured as a marker of apoptosis using the Apo-ONE Homogenous Caspase 3/7 Assay kit. This kit lyses cells in the presence of the caspase 3/7-specific substrate Z-DEVD-R110, which becomes fluorescent once caspases remove the DEVD peptide. We measured fluorescence at an excitation wavelength of 485 nm and emission wavelength of 530 nm with a BioTek Cytation 3 plate reader.

Oxygen consumption—The Oroboros Oxygraph-2k was used to measure oxygen consumption flux as a direct measurement of mitochondrial metabolism. The Oxygraph-2k has two chambers with separate oxygen probes to allow analysis of oxygen consumption of cells in suspension. The instrument was set to a temperature of 37°C, and the stirring speed for each chamber was 500 rpm. To perform these experiments, H4IIEC3 cells were cultured on 6-cm dishes until 80-90% confluent and subsequently incubated with selected treatments for 6 hours. Cells were then trypsinized, counted, and resuspended in the same culture medium and injected into the Oxygraph instrument.

Knockdown of *Glud1*, *GOT1*, and *GOT2*—Small interfering RNA (siRNA) oligonucleotides for *Glud1*, *GOT1*, and *GOT2* were purchased from Integrated DNA Technologies. Cells were treated with 25 nM of selected siRNA complexed to RNAiMAX (Invitrogen) in antibiotic-free DMEM. After 24 hours, complex-containing media was replaced with antibiotic-free DMEM. Following another 24 hours, experiments were performed. Knockdown efficiencies used for selection of siRNA targeting sequences are shown in SI Figure S4.

Polar metabolite extraction and GC-MS analysis of ^{13}C enrichment—Intracellular metabolites from H4IIEC3 rat hepatomas were extracted as previously described (14). Briefly, intracellular metabolism was quenched with 1 mL of -80°C methanol, and cells were scraped into a

mixture of 1:1:1 chloroform, methanol, and water. After drying the aqueous phase, samples were derivatized with MBTSTFA + 1% TBDMCS (Pierce). ^{13}C isotopic enrichment was then analyzed with an Agilent 7890A/5975C GC-MS equipped with a 30m DB-35ms capillary column.

^{13}C metabolic flux analysis (MFA)— ^{13}C MFA was performed using the INCA software package (39) by adapting a previously developed model of hepatocyte metabolism comprising glycolysis, CAC, and anaplerotic pathways (19). This model was updated to include the PEPCK-mediated conversion of oxaloacetate (OAA) to phosphoenolpyruvate (PEP) due to significant labeling observed in PEP. Fluxes were estimated a minimum of 50 times starting from random initial values to identify a global best-fit solution. Once this solution was achieved, a chi-square test was used to assess the goodness-of-fit. Additionally, 95% confidence intervals were calculated for all estimated fluxes by assessing the sensitivity of the sum-of-squared residuals to parameter variations (40). Comprehensive tables of ^{13}C flux results and a detailed description of our network model and assumptions are available in the Supporting Information.

Statistical Analysis—Tests for statistical significance were performed using analysis of variance (Model I ANOVA) and Tukey-Kramer methods for multiple comparisons, or Student's t-test for pair-wise comparisons. Plots indicate +/- one standard error of the mean unless otherwise indicated.

ACKNOWLEDGMENTS

This work was supported by NSF CAREER award CBET-0955251 and NIH R01 DK106348 (to JDY). RAE and SAS were supported by the NSF Graduate Research Fellowship Program. MS was supported by R01 DK060667.

CONFLICT OF INTEREST

The authors declare that they have no conflicts of interest with the contents of this article. The content is solely the responsibility of the authors and does not necessarily represent the official views of the National Institutes of Health.

AUTHOR CONTRIBUTIONS

RAE, AKL, MS, and JDY contributed to the conception and design of experiments. RAE, AKL, SAS, YEC, and MS contributed to data acquisition. RAE, AKL, SAS, and YEC analyzed and interpreted data. RAE, SAS, and JDY drafted the manuscript. All authors contributed to revising the manuscript for critically important intellectual content. All authors approved the manuscript for publication.

REFERENCES

1. Serviddio, G., Bellanti, F., Tamborra, R., Rollo, T., Romano, A. D., Giudetti, A. M., Capitanio, N., Petrella, A., Vendemiale, G., and Altomare, E. (2008) Alterations of hepatic ATP homeostasis and respiratory chain during development of non-alcoholic steatohepatitis in a rodent model. *European Journal of Clinical Investigation* **38**
2. Perez-Carreras, M., Del Hoyo, P., Martin, M. A., Rubio, J. C., Martin, A., Castellano, G., Colina, F., Arenas, J., and Solis-Herruzo, J. A. (2003) Defective hepatic mitochondrial respiratory chain in patients with nonalcoholic steatohepatitis. *Hepatology* **38**
3. Sanyal, A. J., Campbell-Sargent, C., Mirshahi, F., Rizzo, W. B., Contos, M. J., Sterling, R. K., Luketic, V. A., Shiffman, M. L., and Clore, J. N. (2001) Nonalcoholic steatohepatitis: Association of insulin resistance and mitochondrial abnormalities. *Gastroenterology* **120**, 1183-1192
4. Satapati, S., Sunny, N. E., Kucejova, B., Fu, X. R., He, T. T., Mendez-Lucas, A., Shelton, J. M., Perales, J. C., Browning, J. D., and Burgess, S. C. (2012) Elevated TCA cycle function in the pathology of diet-induced hepatic insulin resistance and fatty liver. *Journal of Lipid Research* **53**, 1080-1092
5. Sunny, N. E., Parks, E. J., Browning, J. D., and Burgess, S. C. (2011) Excessive hepatic mitochondrial TCA cycle and gluconeogenesis in humans with nonalcoholic fatty liver disease. *Cell Metab* **14**, 804-810
6. Li, Z. Z., Berk, M., McIntyre, T. M., and Feldstein, A. E. (2009) Hepatic Lipid Partitioning and Liver Damage in Nonalcoholic Fatty Liver Disease ROLE OF STEAROYL-CoA DESATURASE. *Journal of Biological Chemistry* **284**, 5637-5644
7. Puri, P., Baillie, R. A., Wiest, M., Mirshahi, F., and Sanyal, A. J. (2006) A lipidomic analysis of non-alcoholic fatty liver disease (NAFLD). *J. Hepatol.* **44**, S260-S261
8. Li, H., Wang, L., Yan, X., Liu, Q., Yu, C., Wei, H., Li, Y., Zhang, X., He, F., and Jiang, Y. (2011) A Proton Nuclear Magnetic Resonance Metabonomics Approach for Biomarker Discovery in Nonalcoholic Fatty Liver Disease. *Journal of Proteome Research* **10**, 2797-2806
9. Boulangé, C. L., Claus, S. P., Chou, C. J., Collino, S., Montoliu, I., Kochhar, S., Holmes, E., Rezzi, S., Nicholson, J. K., Dumas, M. E., and Martin, F.-P. J. (2013) Early Metabolic Adaptation in C57BL/6 Mice Resistant to High Fat Diet Induced Weight Gain Involves an Activation of Mitochondrial Oxidative Pathways. *Journal of Proteome Research* **12**, 1956-1968
10. Newgard, C. B., An, J., Bain, J. R., Muehlbauer, M. J., Stevens, R. D., Lien, L. F., Haqq, A. M., Shah, S. H., Arlotto, M., Slentz, C. A., Rochon, J., Gallup, D., Ilkayeva, O., Wenner, B. R., Yancy Jr, W. S., Eisenson, H., Musante, G., Surwit, R. S., Millington, D. S., Butler, M. D., and Svetkey, L. P. (2009) A Branched-Chain Amino Acid-Related Metabolic Signature that Differentiates Obese and Lean Humans and Contributes to Insulin Resistance. *Cell Metabolism* **9**, 311-326
11. Cheng, S., Rhee, E. P., Larson, M. G., Lewis, G. D., McCabe, E. L., Shen, D., Palma, M. J., Roberts, L. D., Dejam, A., Souza, A. L., Deik, A. A., Magnusson, M., Fox, C. S., O'Donnell, C. J., Vasan, R. S., Melander, O., Clish, C. B., Gerszten, R. E., and Wang, T. J. (2012) Metabolite Profiling Identifies Pathways Associated With Metabolic Risk in Humans. *Circulation* **125**, 2222-2231
12. Soga, T., Sugimoto, M., Honma, M., Mori, M., Igarashi, K., Kashikura, K., Ikeda, S., Hirayama, A., Yamamoto, T., Yoshida, H., Otsuka, M., Tsuji, S., Yatomi, Y., Sakuragawa, T., Watanabe, H., Nihei, K., Saito, T., Kawata, S., Suzuki, H., Tomita, M., and Suematsu, M. (2011) Serum metabolomics reveals γ -glutamyl dipeptides as biomarkers for discrimination among different forms of liver disease. *J. Hepatol.* **55**, 896-905
13. Sookoian, S., and Pirola, C. J. (2012) Alanine and aspartate aminotransferase and glutamine-cycling pathway: Their roles in pathogenesis of metabolic syndrome. *World Journal of Gastroenterology* **18**, 3775-3781

14. Noguchi, Y., Young, J., Aleman, J., Hansen, M., Kelleher, J., and Stephanopoulos, G. (2009) Effect of Anaplerotic Fluxes and Amino Acid Availability on Hepatic Lipoapoptosis. *Journal of Biological Chemistry* **284**, 33425-33436
15. Egnatchik, R. A., Leamy, A. K., Jacobson, D. A., Shiota, M., and Young, J. D. (2014) ER calcium release promotes mitochondrial dysfunction and hepatic cell lipotoxicity in response to palmitate overload. *Molecular Metabolism* **3**, 544-553
16. Egnatchik, R. A., Leamy, A. K., Noguchi, Y., Shiota, M., and Young, J. D. (2014) Palmitate-induced Activation of Mitochondrial Metabolism Promotes Oxidative Stress and Apoptosis in H4IIEC3 Rat Hepatocytes. *Metabolism: clinical and experimental* **63**, 283-295
17. Satapati, S., Kucejova, B., Duarte, J. A., Fletcher, J. A., Reynolds, L., Sunny, N. E., He, T., Nair, L. A., Livingston, K., Fu, X., Merritt, M. E., Sherry, A. D., Malloy, C. R., Shelton, J. M., Lambert, J., Parks, E. J., Corbin, I., Magnuson, M. A., Browning, J. D., and Burgess, S. C. (2015) Mitochondrial metabolism mediates oxidative stress and inflammation in fatty liver. *J Clin Invest* **125**, 4447-4462
18. Miller, R. A., Shi, Y., Lu, W., Pirman, D. A., Jatkar, A., Blatnik, M., Wu, H., Cardenas, C., Wan, M., Foskett, J. K., Park, J. O., Zhang, Y., Holland, W. L., Rabinowitz, J. D., and Birnbaum, M. J. (2018) Targeting hepatic glutaminase activity to ameliorate hyperglycemia. *Nature medicine* **24**, 518-524
19. Egnatchik, R. A., Leamy, A. K., Noguchi, Y., Shiota, M., and Young, J. D. (2013) Palmitate-induced Activation of Mitochondrial Metabolism Promotes Oxidative Stress and Apoptosis in H4IIEC3 Rat Hepatocytes. *Metabolism: clinical and experimental*
20. Cheng, X., Kim, S. Y., Okamoto, H., Xin, Y., Yancopoulos, G. D., Murphy, A. J., and Gromada, J. (2018) Glucagon contributes to liver zonation. *Proc Natl Acad Sci U S A* **115**, E4111-E4119
21. Brosnan, M. E., and Brosnan, J. T. (2009) Hepatic glutamate metabolism: a tale of 2 hepatocytes. *The American Journal of Clinical Nutrition* **90**, 857S-861S
22. Matsuno, T., and Goto, I. (1992) Glutaminase and glutamine synthetase activities in human cirrhotic liver and hepatocellular carcinoma. *Cancer Res* **52**, 1192-1194
23. Contreras, L., and Satrustegui, J. (2009) Calcium Signaling in Brain Mitochondria INTERPLAY OF MALATE ASPARTATE NADH SHUTTLE AND CALCIUM UNIPORTER/MITOCHONDRIAL DEHYDROGENASE PATHWAYS. *Journal of Biological Chemistry* **284**, 7091-7099
24. Gellerich, F. N., Gizatullina, Z., Trumbeckaite, S., Nguyen, H. P., Pallas, T., Arandarcikaite, O., Vielhaber, S., Seppet, E., and Striggow, F. (2010) The regulation of OXPHOS by extramitochondrial calcium. *Biochimica Et Biophysica Acta-Bioenergetics* **1797**, 1018-1027
25. He, L., Weber, K. J., and Schilling, J. D. (2016) Glutamine Modulates Macrophage Lipotoxicity. *Nutrients* **8**, 215
26. Listenberger, L. L., Ory, D. S., and Schaffer, J. E. (2001) Palmitate-induced Apoptosis Can Occur Through a Ceramide-independent Pathway. *The Journal of Biological Chemistry* **276**, 14890-14895
27. Akagi, S., Kono, N., Ariyama, H., Shindou, H., Shimizu, T., and Arai, H. (2016) Lysophosphatidylcholine acyltransferase 1 protects against cytotoxicity induced by polyunsaturated fatty acids. *The FASEB Journal* **30**, 2027-2039
28. Zhao, N., Li, X., Feng, Y., Han, J., Feng, Z., Li, X., and Wen, Y. (2018) The Nuclear Orphan Receptor Nur77 Alleviates Palmitate-induced Fat Accumulation by Down-regulating G0S2 in HepG2 Cells. *Scientific Reports* **8**
29. Bode, B. P. (2001) Recent Molecular Advances in Mammalian Glutamine Transport. *The Journal of Nutrition* **131**, 2475S-2485S
30. Han, S. J., Choi, S. E., Yi, S. A., Jung, J. G., Jung, I. R., Shin, M., Kang, S., Oh, H., Kim, H. J., Kim, D. J., Kwon, J. E., Choi, C. S., Lee, K. W., and Kang, Y. (2016) Glutamate dehydrogenase

- activator BCH stimulating reductive amination prevents high fat/high fructose diet-induced steatohepatitis and hyperglycemia in C57BL/6J mice. *Scientific reports* **5**, 37468
31. Holzer, R. G., Park, E.-J., Li, N., Tran, H., Chen, M., Choi, C., Solinas, G., and Karin, M. (2011) Saturated fatty acids induce c-Src clustering within membrane subdomains leading to JNK activation. *Cell* **147**, 173-184
32. Cho, C.-S., Park, H.-W., Ho, A., Semple, I. A., Kim, B., Jang, I., Park, H., Reilly, S., Saltiel, A. R., and Lee, J. H. (2018) Lipotoxicity induces hepatic protein inclusions through TANK binding kinase 1-mediated p62/sequestosome 1 phosphorylation. *Hepatology*
33. Park, H.-W., Park, H., Semple, I. A., Jang, I., Ro, S.-H., Kim, M., Cazares, V. A., Stuenkel, E. L., Kim, J.-J., Kim, J. S., and Lee, J. H. (2014) Pharmacological correction of obesity-induced autophagy arrest using calcium channel blockers. *Nature Communications* **5**
34. Fernandez, C. A., Des Rosiers, C., Previs, S. F., David, F., and Brunengraber, H. (1996) Correction of ¹³C mass isotopomer distributions for natural stable isotope abundance. *J Mass Spectrom* **31**, 255-262
35. Zhou, Y., Oresic, M., Leivonen, M., Gopalacharyulu, P., Hyysalo, J., Arola, J., Verrijken, A., Francque, S., Van Gaal, L., Hyotylainen, T., and Yki-Jarvinen, H. (2016) Noninvasive Detection of Nonalcoholic Steatohepatitis Using Clinical Markers and Circulating Levels of Lipids and Metabolites. *Clinical gastroenterology and hepatology : the official clinical practice journal of the American Gastroenterological Association* **14**, 1463-1472 e1466
36. Shiota, M., Inagami, M., Fujimoto, Y., Moriyama, M., Kimura, K., and Sugano, T. (1995) Cold acclimation induces zonal heterogeneity in gluconeogenic responses to glucagon in rat liver lobule. *American Journal of Physiology* **268**, E1184-E1191
37. Qi, Y., Wang, W., Chen, J., Dai, L., Kaczorowski, D., Gao, X., and Xia, P. (2015) Sphingosine Kinase 1 Protects Hepatocytes from Lipotoxicity via Down-regulations of IRE1 α Protein Expression. *The Journal of Biological Chemistry* **290**, 23282-23290
38. Park, H.-W., Park, H., Ro, S.-H., Jang, I., Semple, I. A., Kim, D. N., Kim, M., Nam, M., Zhang, D., Yin, L., and Lee, J. H. (2014) Hepatoprotective role of Sestrin3 against chronic ER stress. *Nature Communications* **5**
39. Young, J. D. (2014) INCA: a computational platform for isotopically non-stationary metabolic flux analysis. *Bioinformatics* **30**, 1333-1335
40. Antoniewicz, M. R., Kelleher, J. K., and Stephanopoulos, G. (2006) Determination of confidence intervals of metabolic fluxes estimated from stable isotope measurements. *Metab Eng* **8**, 324-337

ABBREVIATIONS AND NOMENCLATURE

α KG, alpha-ketoglutarate; ADH, alpha-ketoglutarate dehydrogenase; AOA, aminooxyacetic acid; APE, atom percent enrichment; BSA, bovine serum albumin; CAC, citric acid cycle; CS, citrate synthase; DMEM, Dulbecco's modified Eagle's medium; FFA, free fatty acid; GLS, glutaminase; GOT, glutamate-oxaloacetate transaminase; GPT, glutamate-pyruvate transaminase; MCD, methionine-choline deficient; ME, malic enzyme; MFA, metabolic flux analysis; MID, mass isotopomer distribution; NAFLD, nonalcoholic fatty liver disease; NASH, nonalcoholic steatohepatitis; NEAA, nonessential amino acid; OAA, oxaloacetate; PA, palmitate; PC, pyruvate carboxylase; PEP, phosphoenolpyruvate; PEPCK, phosphoenolpyruvate carboxykinase; PI, propidium iodide; PK, pyruvate kinase.

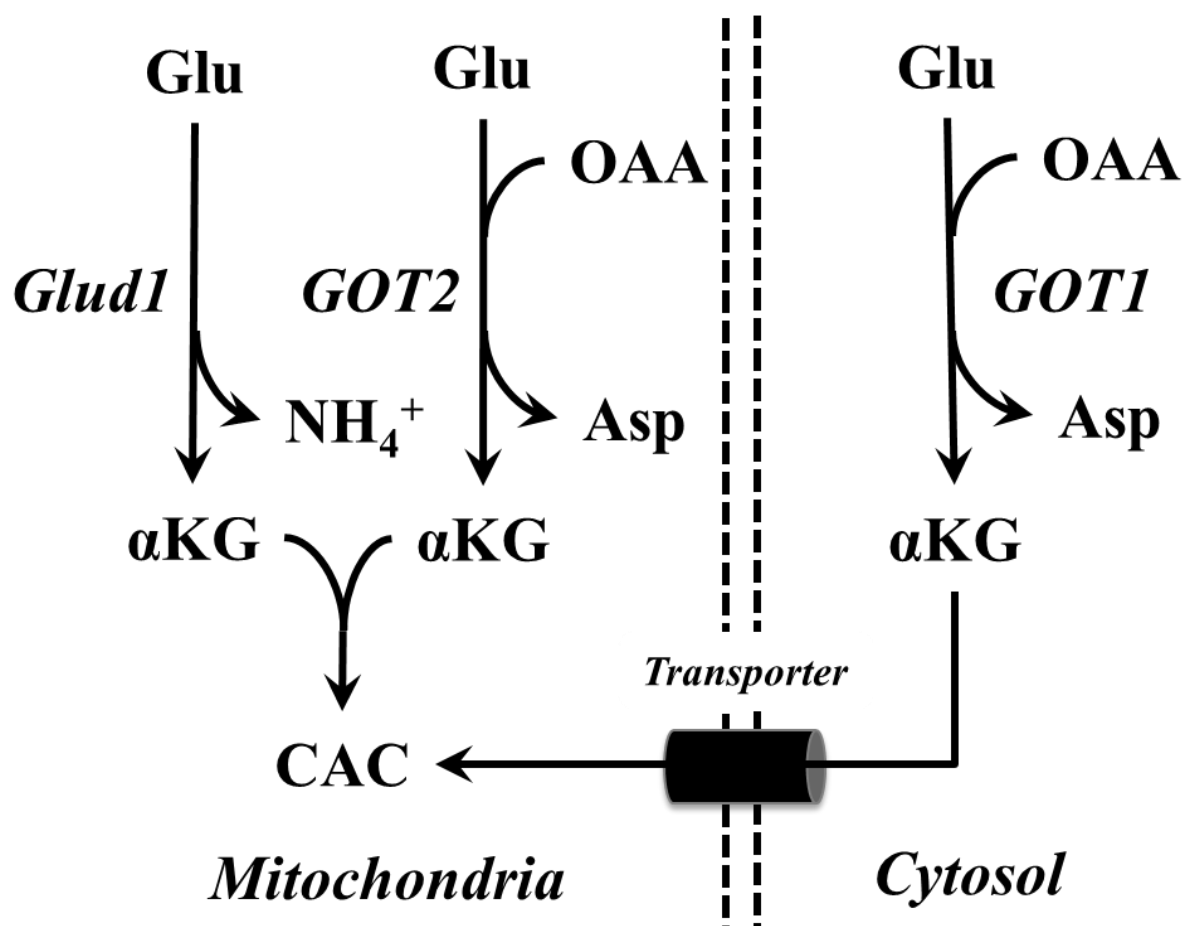


Figure 1. Routes of α -ketoglutarate production leading to CAC anaplerosis. Extracellular glutamine is metabolized in the mitochondria to glutamate (Glu) by the enzyme glutaminase. Glutamate can be metabolized through glutamate dehydrogenase (*Glud1*) or glutamate oxaloacetate transaminase 2 (*GOT2*) to mitochondrial α -ketoglutarate (α KG). Similarly, glutamate oxaloacetate transaminase 1 (*GOT1*) produces cytosolic α KG from Glu, which must then be transported (through a malate/ α KG antiporter) across the mitochondrial inner membrane to enter CAC metabolism. The GOT pathways additionally consume oxaloacetate (OAA) and produce aspartate (Asp).

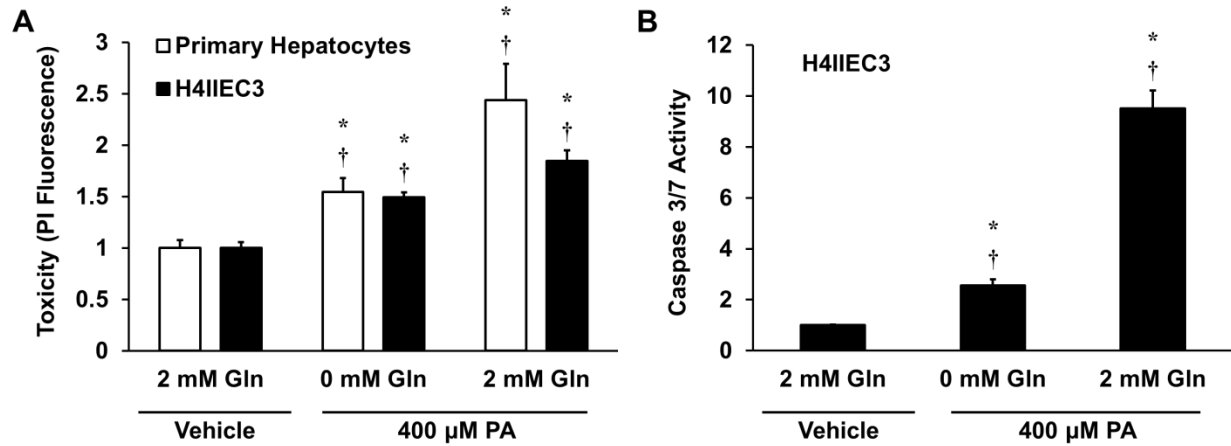


Figure 2. Removal of extracellular glutamine attenuates lipotoxicity. Primary rat hepatocytes and H4IIEC3 cells were treated with 400 μ M palmitate (PA), either in the presence (2 mM) or absence of glutamine (Gln). (A) Cell toxicity assessed by PI fluorescence after 24 hours of treatment. (B) Caspase activity in H4IIEC3 cells after 12 hours of treatment. In both panels, measurements are normalized to BSA (vehicle)-treated cells cultured with 2 mM glutamine. Data represent mean \pm S.E., $n=4$; * different from vehicle, $p < 0.05$, † different from each other (comparison to cells of same type), $p < 0.05$.

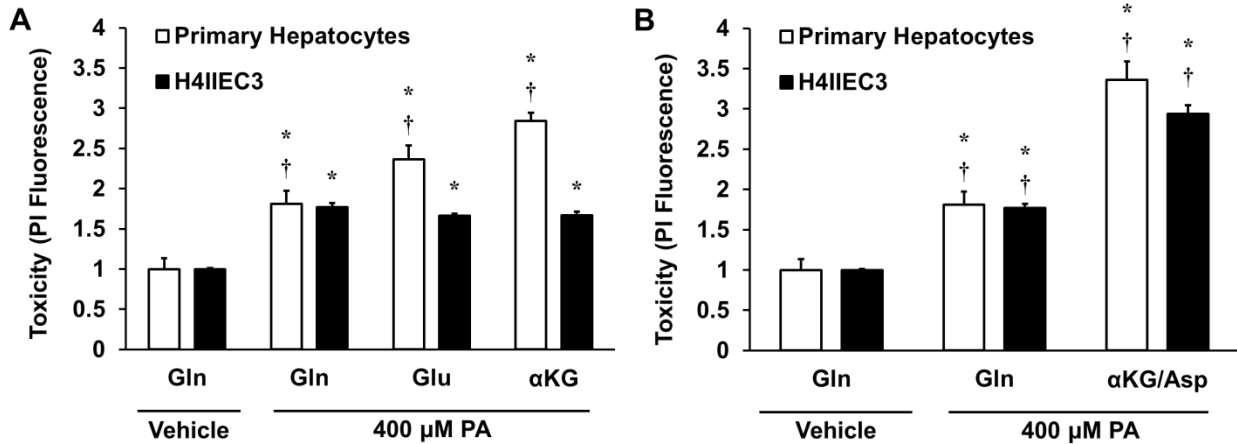


Figure 3. Effects of replacing medium glutamine with downstream products of glutamine metabolism. (A) Primary rat hepatocytes or H4IIEC3 cells were treated with 400 μM palmitate (PA) and cultured with 2 mM glutamine (Gln), glutamate (Glu), or α-ketoglutarate (αKG). Cell death was assessed by PI fluorescence at 24 hours. (B) Relative cell death after 24 hours of treatment with palmitate in the presence of 2 mM glutamine or a mixture of 1 mM α-ketoglutarate and 1 mM aspartate (αKG/Asp). In both panels, PI fluorescence of palmitate-treated cells is normalized to BSA (vehicle)-treated cells cultured with 2 mM glutamine. Data represent mean +/- S.E., n=4; * different from vehicle, $p < 0.05$, † different from each other (comparison to cells of same type), $p < 0.05$.

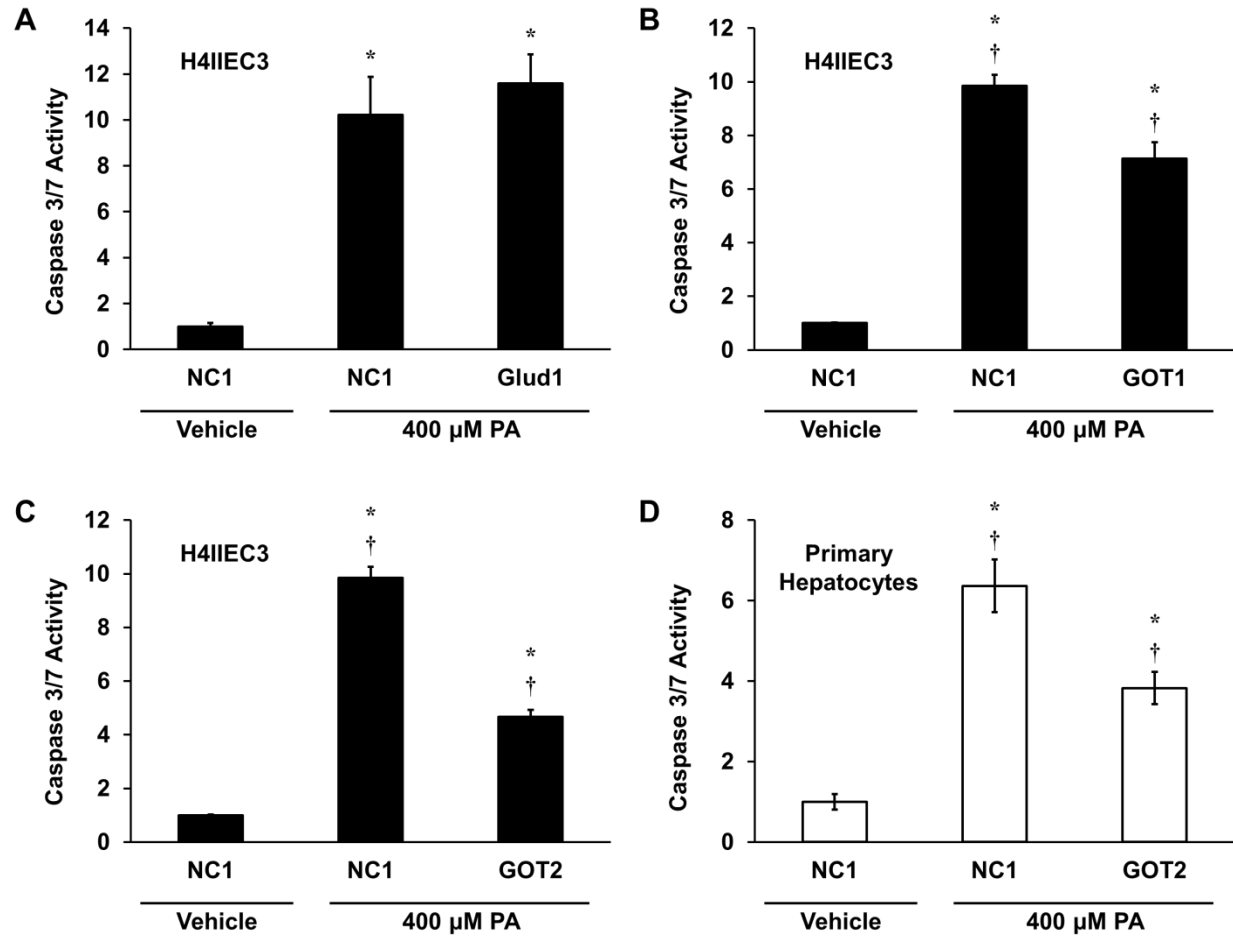


Figure 4. GOT activity promotes glutamine-dependent palmitate lipotoxicity. H4IIEC3 cells were transfected with control siRNA (NC1) or siRNA specific for (A) Glut1, (B) GOT1, or (C) GOT2 and assayed for markers of apoptosis after 12 hours of treatment with 400 μ M palmitate (PA). (D) Primary rat hepatocytes were transfected with control siRNA (NC1) or GOT2 siRNA and assayed for markers of apoptosis after 12 hours of treatment with 400 μ M palmitate (PA). All palmitate-treated conditions are normalized to BSA-treated (vehicle) cells transfected with control siRNA. Data represent the mean \pm S.E., n=4; * different from vehicle, p < 0.05, † different from each other, p < 0.05.

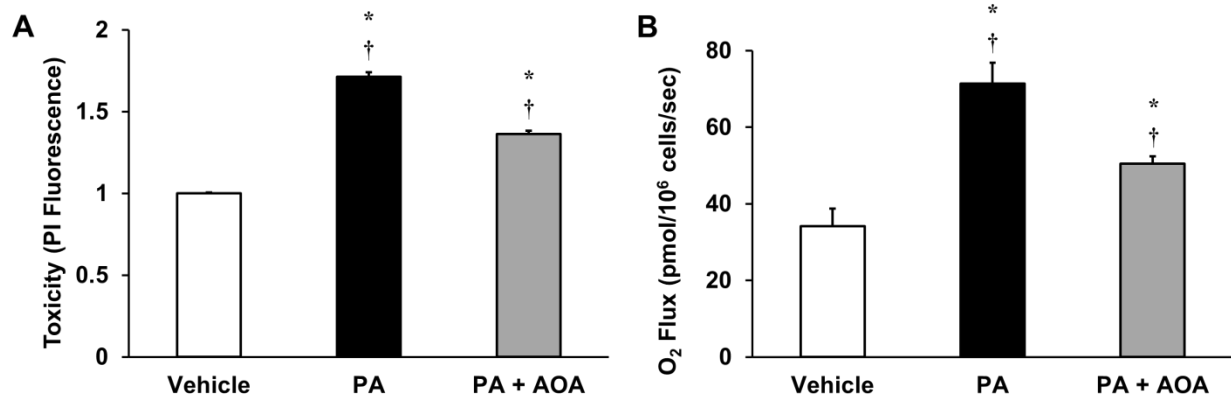


Figure 5. AOA reduces palmitate-induced cell death and activation of oxidative metabolism. H4IIEC3 cells were treated with 400 μ M palmitate in combination with 500 μ M of the transaminase inhibitor AOA (PA + AOA) and compared to palmitate-treated (PA) cells. (A) Cell toxicity was assessed after 24 hours of treatment and normalized to BSA (vehicle)-treated conditions. (B) Oxygen consumption rates of H4IIEC3 cells treated with vehicle, PA, or PA+AOA were measured after 6 hours of treatment. Data represent mean \pm S.E., $n=4$ for toxicity, $n=3$ for oxygen uptake; *different from vehicle, $p < 0.05$, † different from each other, $p < 0.05$.

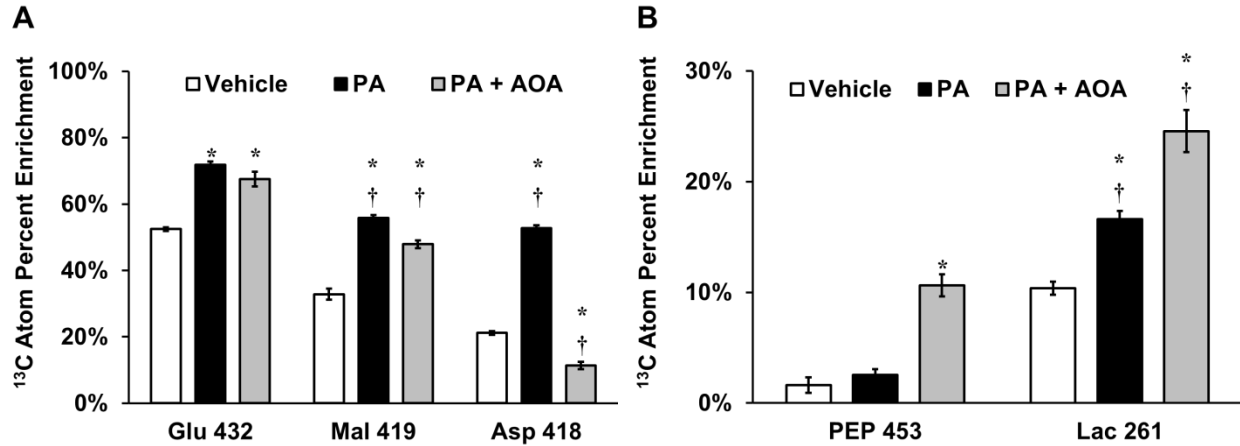


Figure 6. Isotopic enrichments of intracellular metabolites indicate flux re-routing in response to AOA treatment. Unlabeled medium glutamine was replaced with [U-¹³C₅]glutamine and used to isotopically enrich H4IIEC3 cells treated with vehicle (BSA), 400 μM palmitate (PA), or a combination of 400 μM palmitate and 500 μM AOA (PA + AOA). After extraction and GC-MS analysis of intracellular metabolites, mass isotopomer distributions (MIDs) were corrected for natural isotope abundance using the method of Fernandez et al. (34). Atom percent enrichment (APE) of selected metabolites was calculated using the formula

$$APE = 100\% \times \sum_{i=0}^N \frac{M_i \times i}{N},$$

where N is the number of carbon atoms in the metabolite and M_i is the fractional abundance of the i th mass isotopomer of the metabolite. APE provides a measure of the fractional synthesis of a metabolite from the isotope tracer (i.e., glutamine) relative to unlabeled carbon sources (e.g., glucose). The fragment ions analyzed for APE were (A) Glu 432, Mal 419, Asp 418, and (B) PEP 453, Lac 261. These ions contain the full carbon backbone of their associated parent metabolites (i.e., $N=5$ for glutamate, $N=4$ for malate and aspartate, and $N=3$ for PEP and lactate). Data represent mean \pm S.E., $n=3$; * different from vehicle, $p < 0.05$, † different from each other, $p < 0.05$.

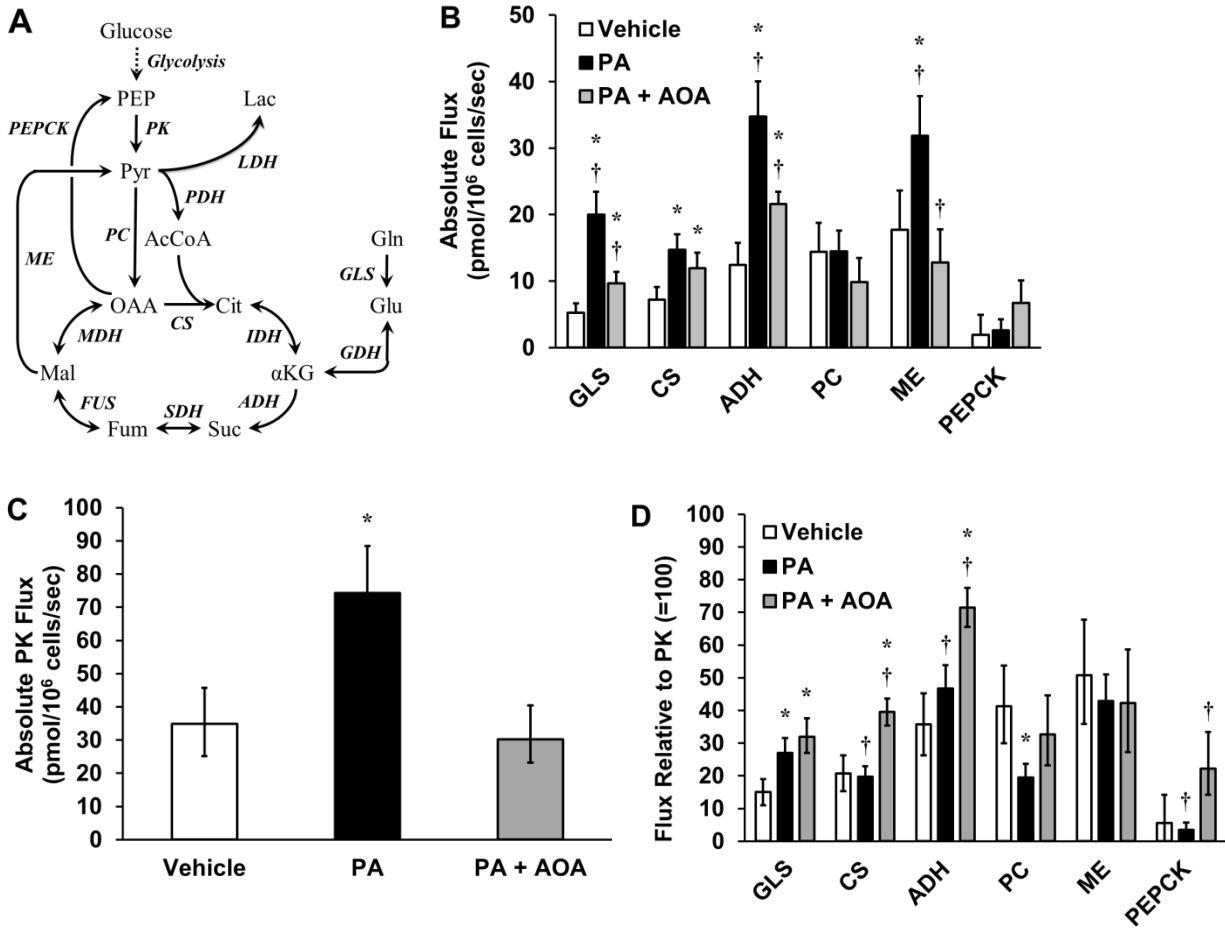


Figure 7. ¹³C MFA reveals that AOA treatment reduces mitochondrial fluxes and re-routes malic enzyme flux in the presence of palmitate. (A) Reaction network used for ¹³C flux analysis. (B) Absolute intracellular CAC fluxes were determined for H4IIEC3 cells treated with BSA (vehicle), 400 μ M palmitate (PA), or a combination of 400 μ M palmitate and 500 μ M AOA (PA + AOA). (C) Estimated pyruvate kinase (PK) flux in each treatment condition. (D) Relative fluxes (normalized to PK=100) demonstrate that AOA co-treatment is associated with enhanced glutamate anaplerosis, despite a reduction in absolute mitochondrial fluxes. Abbreviations: GLS=glutaminase, GDH=glutamate dehydrogenase (includes both GOT and Glud1 activity), CS=citrate synthase, IDH=isocitrate dehydrogenase, ADH= α -ketoglutarate dehydrogenase, SDH=succinate dehydrogenase, FUS=fumarase, MDH=malate dehydrogenase, PC=pyruvate carboxylase, ME=malic enzyme, PEPCK=PEP carboxykinase, PK=pyruvate kinase, PDH=pyruvate dehydrogenase, LDH=lactate dehydrogenase. Error bars indicate 95% confidence intervals; * different from vehicle, $p < 0.05$, † different from each other (comparison to same flux across different treatments), $p < 0.05$.

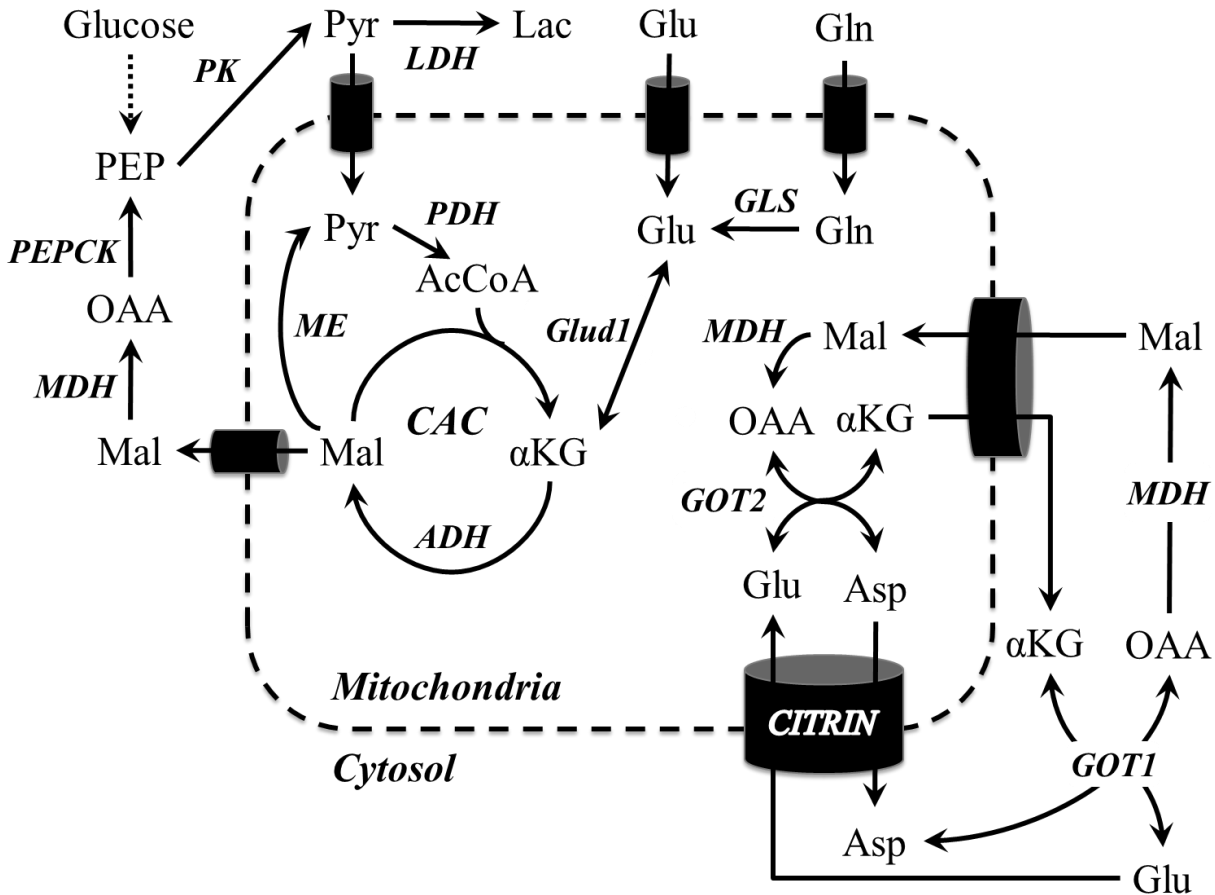


Figure 8. Metabolic pathways and putative mechanisms investigated in this study. Pathways of α KG anaplerosis were inhibited using siRNA and the pharmacological inhibitor AOA. GOT2 metabolism potentiated lipoapoptosis more than other anaplerotic mechanisms. Additionally, simultaneous inhibition of GOT1/GOT2 with AOA suppressed lipotoxic dysregulations of mitochondrial metabolism. Combined with prior work, these results also suggest a possible role for the glutamate/aspartate antiporter citrin and the CAC enzyme α -ketoglutarate dehydrogenase (ADH), both of which are known to potentiate calcium-stimulated mitochondrial metabolism of glutamate.

Glutamate-oxaloacetate transaminase activity promotes palmitate lipotoxicity in rat hepatocytes by enhancing anaplerosis and citric acid cycle flux

Robert A. Egnatchik, Alexandra K. Leamy, Sarah A. Sacco, Yi Ern Cheah, Masakazu Shiota and Jamey D. Young

J. Biol. Chem. published online December 18, 2018

Access the most updated version of this article at doi: [10.1074/jbc.RA118.004869](https://doi.org/10.1074/jbc.RA118.004869)

Alerts:

- [When this article is cited](#)
- [When a correction for this article is posted](#)

[Click here](#) to choose from all of JBC's e-mail alerts